

See discussions, stats, and author profiles for this publication at: <https://www.researchgate.net/publication/302070360>

The integrated ocean dynamics and acoustics project

Article in The Journal of the Acoustical Society of America · April 2016

DOI: 10.1121/1.4949977

CITATIONS

0

READS

303

24 authors, including:



[Weifeng G. Zhang](#)

Woods Hole Oceanographic Institution

33 PUBLICATIONS 345 CITATIONS

[SEE PROFILE](#)



[John Wilkin](#)

Rutgers, The State University of New Jersey

92 PUBLICATIONS 2,849 CITATIONS

[SEE PROFILE](#)



[Pierre F. J. Lermusiaux](#)

Massachusetts Institute of Technology

130 PUBLICATIONS 2,800 CITATIONS

[SEE PROFILE](#)



[Mohsen Badiy](#)

University of Delaware

266 PUBLICATIONS 1,535 CITATIONS

[SEE PROFILE](#)

All content following this page was uploaded by [Pierre F. J. Lermusiaux](#) on 01 August 2016.

The user has requested enhancement of the downloaded file. All in-text references [underlined in blue](#) are added to the original document and are linked to publications on ResearchGate, letting you access and read them immediately.

THE “INTEGRATED OCEAN DYNAMICS AND ACOUSTICS” (IODA) HYBRID MODELING EFFORT

Timothy F. Duda^a, Ying-Tsong Lin^a, Arthur E. Newhall^a, Karl R. Helfrich^a,
Weifeng Gordon Zhang^a, Mohsen Badiey^b, Pierre F.J. Lermusiaux^c,
John A. Colosi^d, and James F. Lynch^a

^a Woods Hole Oceanographic Institution, Woods Hole, MA 02543 USA

^b University of Delaware, Newark, DE 19716 USA

^c Dept. of Mechanical Engineering, Massachusetts Institute of Technology, Cambridge,
MA 02139 USA

^d Oceanography Department, Naval Postgraduate School, Monterey, CA 93943 USA

Contact author: T. F. Duda, WHOI Applied Ocean Physics and Engineering Dept., MS 11,
Woods Hole, MA, 02543 USA; fax +1 508 457 2194; tduda@whoi.edu

Abstract: *Regional ocean models have long been integrated with acoustic propagation and scattering models, including work in the 1990s by Robinson and Lee. However, the dynamics in these models has been not inclusive enough to represent submesoscale features that are now known to be very important acoustically. The features include internal waves, thermohaline intrusions, and details of fronts. In practice, regional models predict internal tides at many locations, but the nonlinear steepening of these waves and their conversion to short nonlinear waves is often improperly modeled, because computationally prohibitive nonhydrostatic pressure is needed. To include the small-scale internal waves of tidal origin, a nested hybrid model is under development. The approach is to extract long-wavelength internal tide wave information from tidally forced regional models, use ray methods or mapping methods to determine internal-tide propagation patterns, and then solve two-dimensional high-resolution nonhydrostatic wave models to “fill-in” the internal wave details. The resulting predicted three-dimensional environment is then input to a fully three-dimensional parabolic equation acoustic code. The output from the nested ocean model, run in hindcast mode, is to be compared to field data from the Shallow Water 2006 (SW06) experiment to test and ground truth purposes.*

Keywords: *acoustic propagation modelling, internal tides, nonlinear internal waves, ocean dynamical modelling*

1. INTRODUCTION

The computational modelling of ocean water movement and ocean water property evolution has a history spanning more than 50 years. The rationale for this effort is multifaceted, including prediction, real-time calculation of actual conditions with wide dynamic range, and idealized modelling in order to foster understanding of the physical processes at work. The processes range in scale from climatic to wave-period in duration, and from planetary to pebble-sized in length scale. Here, we present work at medium scales, aimed at features that have been determined to be of interest from an underwater acoustic propagation standpoint, of hours to weeks in duration, and tens of meters to tens of kilometres in length scale.

This work involves the interfacing of so-called regional ocean models, running in data assimilation (DA) mode and covering spatial scales from hundreds of kilometres down to about a kilometre, to models suited to smaller-scale features. In DA mode the model outputs are driven towards reality as much as possible, being typically data-starved by nature [1-2]. Modern data-driven regional models use the hydrostatic pressure assumption, where water vertical acceleration is not fully considered. (Vertical force does not equal mass times acceleration.) Including the nonhydrostatic pressure makes the computation far more intensive.

The reason for interfacing these models is that, through recent research efforts, the community has come to realize that nonlinear internal waves (NIW) of order 100-m wavelength exhibiting nonhydrostatic pressure physics can have profound impacts on sound propagation. These waves can focus energy [3-6], and can affect coherence [7-8], multipath interference [9], and reverberation [10]. However, these waves are not properly handled by the hydrostatic regional models, so their properties can not be predicted simply by extending the data-driven regional modelling approach to smaller scales and periods.

Here, a hybrid (or composite) method for computing highly resolved three-dimensional waves with nonhydrostatic pressure (NP) dynamics within ocean volumes is outlined, where only the longer-wavelength features are modelled in data-driven fashion. The method is aimed at the prediction of NIW that develop from long-wavelength internal waves at tidal frequency (internal tides, IT), which arise in the regional models. The method has not yet been proven to be sufficiently accurate to improve activities like sonar system performance prediction. Making this assessment is one of our research goals. The development and testing of this hybrid model is one component of a larger project, IODA, defined in the title, which also includes basic research in IT formation and dynamics, NP wave dynamics, surface wave modelling, regional model development, statistical and computational acoustic propagation modelling, NP computational modelling, and efficient or optimal interfacing of ocean environment models and acoustic models (i.e. passing sufficiently but not unnecessarily detailed sound-speed structures to acoustic models).

2. THE HYBRID MODEL COMPONENTS

The *first component* is a regional model (RM) running in DA mode with tidal forcing, so that internal tides develop. The mechanism for IT generation is oscillatory flow near a sloped seabed, so that boundary conditions induce oscillatory vertical flow [11]. In deeper waters, IT tend to have small current and displacement amplitudes, thus are linear, and are well approximated as exhibiting hydrostatic pressure (HP) dynamics. In addition, as the IT

move toward shallow water, they can be described by only a few vertical baroclinic flow normal modes.

This leads to the **second component**: a ray-tracing model describing the propagation of IT normal modes. This model requires the modal properties to be computed from the deduced output of the regional model. Required are vertical structures of internal-wave modes (eigenfunctions), with phase speed (c) related to the eigenvalues. It also requires IT initial conditions from the regional model. This component gives IT properties in an area of interest. In some situations, it may be possible to extract the IT properties from the model using filters, but in general it is difficult to separate the IT field from eddy features, particularly moving eddies. This exposes an important caveat for the ray-trace component: The background through which the IT waves propagate does not vary slowly compared to the waves and at scales that are larger than the waves, so ray tracing is not rigorously valid. But it is nonetheless done. The validity of this can be examined by comparing full RM output with de-IT-processed RM output plus traced IT fields. Typically, rays begin where IT waves are found to form (or believed to form).

As stated, the NIW evolve from the internal tides as they propagate [12-13]. This is modelled with the **third component**, a nonlinear wave evolution model with NP dynamics. The most familiar model is the two-dimensional (vertical slice) Korteweg-de Vries model. Here, we use a generalization of KdV, the extended KdV model with earth rotation [14], which we abbreviate as eKdVf. This is a cubic nonlinear equation for internal-wave mode amplitudes in a time-space domain. Writing mode-one amplitude as η , the equation is

$$\frac{d}{ds} \frac{\partial \eta}{\partial t} + (c + \alpha \eta + \alpha_1 \eta^2) \frac{\partial \eta}{\partial s} + \beta \frac{\partial^3 \eta}{\partial s^3} - \frac{c}{Q} \frac{dQ}{ds} \eta = \frac{f^2}{2c} \eta \quad (1)$$

The spatial dimension s is along-ray distance in our scenario. The nonlinear term coefficients (α 's) and the NP-dispersion coefficient (β) are specific to the mode being worked on; they are integrals involving the mode eigenfunctions. Q is a related variable that allows slowly-varying depth. Rotation effects are imparted by f , equal to 2 times latitude times the earth rotation rate. The eKdVf is solved along IT rays to give short-wavelength NIW along the rays. We solve only along mode-one IT rays because mode one dominates on continental shelves [13], our major interest. The along-ray mode-amplitudes $\eta(s, t)$ are then converted to time-dependent 2D along-ray sound-speed fields, and then interpolated to give the evolving 3D sound speed field. The eKdVf solution is a refinement of the IT field present in the RM, and of the IT field calculated with ray tracing, so these are not passed on to the fourth and final component.

The **fourth component** of the model is a 3D parabolic equation sound propagation code [15]. This is run sequentially in time to produce evolving sonic fields, which we call 3.5D modelling (as opposed to true 4D modelling of sound in moving water).

3. DEMONSTRATION OF SIMULATION OUTPUT

The modelling is perhaps better understood by viewing examples of the outputs. Figure 1 shows fields from the data-assimilative RM [16], developed for real-time predictions in the ONR SW06 experiment, and since refined (reanalysis: improved initial conditions and data; improved resolution). The surface temperature variations (left) illustrate the internal-wave mode speed anomalies and circulation features that the IT, visualized at right, must propagate through. The internal tides are analyzed by projecting vertical profiles of press-

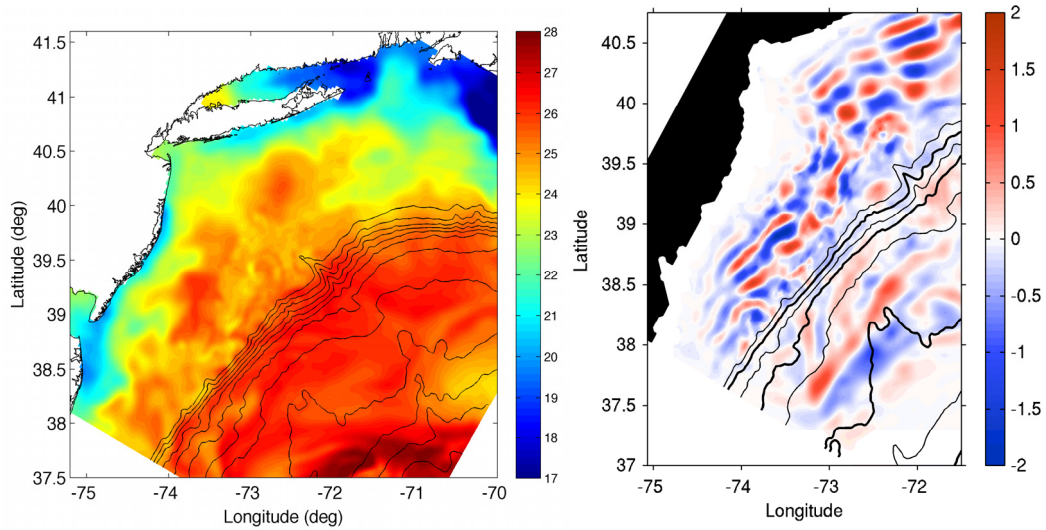


Fig. 1: (left) Surface temperature snapshot from the MIT MSEAS data-assimilative regional model, summer 2006 conditions. (right) A snapshot of 30-m depth semidiurnal-band filtered temperature fluctuations, visualizing ITs that propagate away from the continental-shelf edge (closely bunched contours) in both directions. Initial conditions for an along-ray eKdVf calculation will be similar to a sequence of values of this parameter at the ray origin. IT interference can be seen. The IT in this model propagate through and interact with the complex environment seen at the left, as do ray-traced IT for the hybrid model.

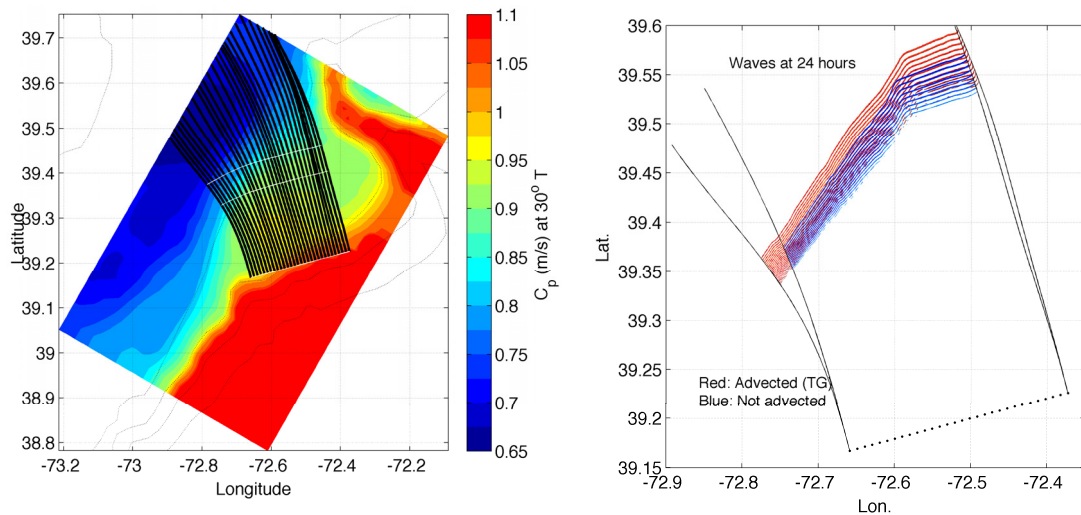


Fig. 2: (left) The mode-1 long wave (asymptotic) internal wave speed for the background 3D model flow field is shown, in color, for one particular wave direction. Mode-1 internal-tide rays starting at a line of hypothetical sources are plotted in black. Two isophase fronts are superimposed in white. (right) Areas of surface current convergence for full-bandwidth nonlinear internal waves simulated with eKdVf are shown for two scenarios. The waves computed with advection taken into account are shown in red; these use the rays shown in the left panel. The waves computed with the background current set to zero are shown in blue.

ure anomaly and/or velocity onto the vertical dynamical normal mode shapes, then Fourier transforming in 62-hour windows to obtain time series records of normal-mode oscillation amplitudes at the resolved frequencies. Oscillations near the diurnal and semidiurnal forcing frequencies dominate. Fig. 1 (right) does not show this analyzed product, but instead simply shows a snapshot of semidiurnal band-passed temperature fluctuations at 30 m. This looks very much like the mode-1 signal because mode-1 is dominant.

Next, the left panel of Fig. 2 shows results of internal-tide ray tracing. Rays are initialized at locations along a line near the critical slope location, which often divides on-shelf IT energy flux from toward-ocean flux. At the critical slope location, semidiurnal internal-wave 3D characteristics, in the horizontal direction parallel with the bathymetric gradient, are parallel with the seabed. Critical locations often run along a line, so the example internal-tide rays start along a line. On the left, the rays are shown, including the effects of advection by sheared currents (functions of x, y , and z) extracted from the model. The IT rays that are shown result from anisotropic ray tracing, using wave speed derivatives in x , y and azimuth (ray direction), which are found by solving the $k=0$ (long-wave) version of the Taylor-Goldstein equation.

On the right of Fig. 2 are snapshots of simulated nonlinear internal waves (mode-one amplitudes) computed by first solving the evolution equation along each ray, then interpolating to fill areas between the rays. Initial conditions are IT sine waves, identical for all rays. Two sets of waves are shown, one computed along IT rays that include advection by currents, and one along rays that ignore current and are controlled only by (x, y) gradients of stratification and water depth. The dark traces show areas of strong surface convergence in waves computed by eKdVf; these are the bright streaks in typical satellite synthetic radar images of internal waves. The currents are seen to push the southern waves to the southwest. A sharp bend appears in the predicted wavefront with or without currents. Importantly, initial conditions in this demonstration are the same for each ray, and are not taken from the RM.

The final step is to feed the internal wave fields to the acoustic PE model. Here, 200 Hz sound is propagated about 8.5 km. The sound approaches the waves from ahead (from the west) then enters the waves. To feed the wave information to the PE, the 2D-interpolated mode-one amplitudes (Fig. 2, right) are first bilinearly interpolated onto a 40 by 40 meter square grid. Then, the demonstration shown here uses a locally representative mode-one shape to build a 3D displacement field, from which a 3D sound-speed field is computed by adjusting depths of a background sound-speed profile, computed from background temperature and salinity profiles. The full model, in development, will use the spatially-dependent background conditions (already used in the wave evolution model) to estimate mode shapes everywhere, and sound-speed profiles everywhere, refining the results. Fig. 3 shows, at the left, the domain where 3D sound-speed is computed, and the acoustic domain. A horizontal planar slice through 3D acoustic field is shown at the right. The PE domain covers only a small portion of the area of the internal-wave simulation (Fig. 3, left).

It is immediately evident from Fig. 3 (right) that the sound propagation has an axisymmetric nature near the source, with a ring pattern of intensity at this depth, explainable by mode interference. Within the internal waves, mode coupling occurs, with mode coupling details being a function of position along the line where the sound enters the waves (the left edge of the waves). This is because the acoustic-source to wave distance varies with the azimuth of these lines, varying the relative mode phases [17].

4. INTRIGUING MODELING ISSUES

The modelling that we have accomplished to date involves a number of approximations, or simplifying assumptions, that need to be validated. (Or abandoned, if necessary.) Chief among these is the consideration of only mode-one internal tides while setting up and running the eKdVf prediction of nonlinear internal waves. The use of mode-one eKdVf solutions to simulate the high-frequency waves is justifiable based on similarity of modelled and observed fields. On the contrary, satellite SAR images suggest that nonlinear waves on the shelf have more complicated spatial patterns than the mode-one ITs that the hydrostatic RM predict. This is because many other internal waves are present in the real ocean which are not resolved nor initialized in the RM (due to lack of measurements). Mode one dynamics along may thus be insufficient for eKdVf initial conditions along rays (not yet implemented in the example, to be clear).

At this time, we plan to use mode-one IT amplitudes along the critical-slope line (looking something like an along-slope isobath) to define likely IT ray starting points, and use IT phase gradients to define ray initial directions. However, field studies [18] and computational studies [19] have shown that internal tides can move upward in beams from the seafloor into the thermocline, with beams being equivalent to multiple modes. Uncoupled normal-mode propagation is a simplification of what actually happens when long-waves of many modes propagate into shallow water, increasing in energy density to the point where nonlinear effects are in play [20]. Because the energy density in the main thermocline must be a determining factor in the generation of thermocline-trapped (mode-one) high-frequency waves, the modal interference behaviour must be relevant. For these reasons, we are considering ways to use a multi-mode model to devise input conditions for the eKdVf. This may be consistent with taking initial condition directly from the RM thermocline dynamics (thus, in addition to using detided RM fields to compute the back-

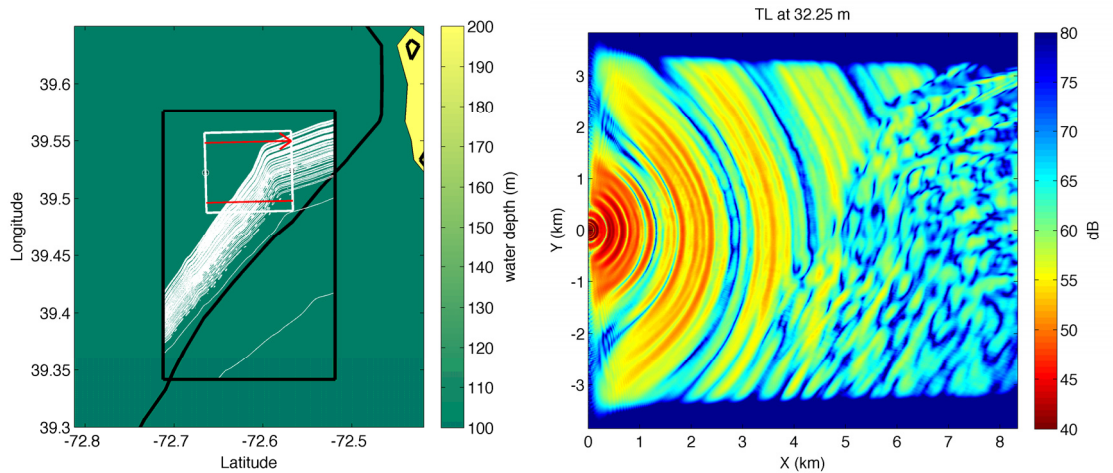


Fig. 3: (left) The area of the Cartesian 3D PE acoustic computation through the internal wave field computed with advection (Taylor-Goldstein, blue in Fig. 2) is shown with a white box. The red arrow indicates that the sound source is at the center of the left box edge; the arrow points in the marching direction. The black box shows interpolated area available for the 3D sound-speed calculation. (right) A snapshot of transmission loss at 32.25 m depth, 200 Hz is plotted. A transition occurs as sound energy enters the waves. The water depth is 80 m at this site, and the internal waves are 20 to 25 m in height.

ground medium for eKdVf-deduced shelf internal tide and waves, using the residual fields for internal-wave initial conditions.). However, the modal content of internal tides may not be well described by the hydrostatic RM with limited bathymetric resolution, so an accurate interference pattern may be challenging to extract.

Another concern is the energy of the nonlinear internal wave field. The waves depicted in Figs. 2 and 3 have higher energies than seen in the field (not shown). The eKdVf model has no dissipation, whereas short nonlinear waves are well known to spawn turbulence and to dissipate as they travel. An empirically-tested wave dissipation scheme may improve the comparison with actual waves. Another possible cause of excess wave energy is the fact that initial conditions seem to cause localized “point” sources of oceanic nonlinear waves, while the scheme presented here does not account for the cylindrical spreading loss that would result. Our current scheme would need an additional inter-ray distance scaling of wave energy to account for spreading loss. This issue of apparent point sources of nonlinear internal waves ties in with the issue of initial condition variability for the mode-one eKdVf along the locus of ray origin points.

5. SUMMARY

The linked ocean mesoscale, internal wave, and acoustic modelling effort is described here, and is demonstrated with a small amount of output. An example computation illustrates the potential of the method for localizing internal waves, and for computing their acoustic effects, in regions spanning thousands of square kilometres. The outstanding technical issues are also discussed, generally regarding the modelling of short wavelength internal waves.

6. ACKNOWLEDGEMENTS

This modelling effort is a component of a Multidisciplinary University Research Initiative research project administered by Dr. Robert Headrick of the Office of Naval Research, USA (Grant number N00014-11-1-0701). Drs. Pat Haley (MIT) and Sam Kelly (at MIT for this work, now at U. Minn. Duluth) are thanked for providing simulation fields.

REFERENCES

- [1] **Lermusiaux, P. F. J., and A. R. Robinson**, Data assimilation via error subspace statistical estimation, Part 1, theory and schemes, *Mon. Wea. Rev.*, vol. 127, pp. 1385-1407, 1999
- [2] **Moore, A. M., H. G. Arango, E. Di Lorenzo, B. D. Cornuelle, A. J. Miller and D. J. Neilson**, A comprehensive ocean prediction and analysis system based on the tangent linear and adjoint of a regional ocean model, *Ocean Modelling*, vol. 7, pp. 227-258, 2004
- [3] **Badiey, M., B. G. Katsnelson, J. F. Lynch, S. Pereselkov, and W. L. Siegmann**, Measurement and modeling of three-dimensional sound intensity variations due to shallow-water internal waves, *J. Acoust. Soc. Am.*, vol. 117, pp. 613-625, 2005

- [4] **Oba, R., and S. Finette**, Acoustic propagation through anisotropic internal wave fields: Transmission loss, cross-range coherence, and horizontal refraction, *J. Acoust. Soc. Am.*, vol. 111, pp. 769–784, 2002
- [5] **S. Finette, S., and R. Oba**, Horizontal array beamforming in an azimuthally anisotropic internal wave field, *J. Acoust. Soc. Am.*, vol. 114, pp. 131–144, 2003
- [6] **Lynch, J. F., Y.-T. Lin, T. F. Duda and A. E. Newhall**, Acoustic ducting, reflection, refraction, and dispersion by curved nonlinear internal waves in shallow water, *IEEE J. Oceanic Eng.*, vol. 35, pp. 12-27, 2010.
- [7] **Collis, J. M., T. F. Duda, J. F. Lynch, and H. A. DeFerrari**, Observed limiting cases of horizontal field coherence and array performance in a time-varying internal wavefield, *J. Acoust. Soc. Am.*, vol. 124, pp. EL97-EL103, 2008.
- [8] **Duda, T. F., J. M. Collis, Y.-T. Lin, A. E. Newhall, J. F. Lynch and H. A. DeFerrari**, Horizontal coherence of low-frequency fixed-path sound in a continental shelf region with internal-wave activity, *J. Acoust. Soc. Am.*, vol. 131, pp. 1782-1797, 2012.
- [9] **Luo, J. and M. Badiéy**, Frequency dependent beating patterns and amplitude increase during the approach of an internal wave packet, *J. Acoust. Soc. Am.*, vol. 131, pp. EL145-EL149, 2012.
- [10] **Heney, F. S. and D. Tang**, Reverberation clutter induced by nonlinear internal waves in shallow water, *J. Acoust. Soc. Am.*, vol. 134, pp. EL289-EL293, 2013.
- [11] **Baines, P. G.**, The generation of internal tides by flat-bump topography, *Deep-Sea Res.*, vol. 20, pp. 179-205, 1973.
- [12] **Lamb, K. G., and L. Yan**, The evolution of internal wave undular bores - comparisons of a fully nonlinear numerical model with weakly nonlinear theory, *J. Phys. Oceanogr.*, vol. 26, pp. 2712- 2734, 1996.
- [13] **Green, J. A. M., J. H. Simpson, S. Legg, and M. R. Palmer**, Internal waves, baroclinic energy fluxes and mixing at the European shelf edge. *Cont. Shelf Res.*, vol. 28, pp. 937–950, 2008.
- [14] **Holloway, P. E., E. Pelinovsky and T. Talipova**, A generalized Korteweg-de Vries model of internal tide transformations in the coastal zone, *J. Geophys. Res.*, vol. 104, pp. 18,333-18,350, 1999
- [15] **Lin, Y.-T., T. F. Duda and A. E. Newhall**, Three-dimensional sound propagation models using the parabolic-equation approximation and the split-step Fourier method, *J. Comput. Acoust.*, vol. 21, p. 1250018, 2013.
- [16] **Haley, P. J., Jr. and P. F. J. Lermusiaux**, Multiscale two-way embedding schemes for free-surface primitive-equations in the Multidisciplinary Simulation, Estimation and Assimilation System, *Ocean Dyn.*, vol. 60, pp. 1497-1537, 2010.
- [17] **Preisig, J. C. and T. F. Duda**, Coupled acoustic mode propagation through continental-shelf internal solitary waves, *IEEE J. Ocean. Eng.*, vol. 22, pp. 256–269, 1997.
- [18] **Duda, T. F., J. F. Lynch, J. D. Irish, R. C. Beardsley, S. R. Ramp, C.-S. Chiu, T. Y. Tang and Y. J. Yang**, Internal tide and nonlinear internal wave behavior at the continental slope in the northern South China Sea, *IEEE J. Oceanic Eng.*, vol. 29, pp. 1105-1130, 2004.
- [19] **Zhang, W. G. and T. F. Duda**, Intrinsic nonlinearity and spectral structure of internal tides at an idealized Mid-Atlantic Bight shelfbreak, *J. Phys. Oceanogr.*, vol. 43, pp. 2641-2660, 2013.
- [20] **Gerkema, T.**, Internal and interfacial tides: Beam scattering and local generation of solitary waves, *J. Mar. Res.*, vol. 59, pp. 227–255, 2001.